Title

Assessment of simulated lesions on primary teeth with near-infrared imaging

Authors

Tam, Wilson

Lee, Robert C

Lin, Brent

et al.

Publication Date

2016-02-29

DOI

10.1117/12.2218660

Peer reviewed

HHS Public Access

Author manuscript

Proc SPIE Int Soc Opt Eng. Author manuscript; available in PMC 2016 March 16.

Published in final edited form as:

Proc SPIE Int Soc Opt Eng. 2016 February 13; 9692: . doi:10.1117/12.2218660.

Assessment of simulated lesions on primary teeth with near-infrared imaging

Wilson Tam, **Robert C. Lee**, **Brent Lin**, **Jacob C. Simon**, and **Daniel Fried**

University of California, San Francisco, San Francisco, CA 94143-0758

Abstract

Previous studies have demonstrated that the structural changes on enamel due to demineralization and remineralization can be exploited through optical imaging methods such as QLF, thermal and NIR imaging. The purpose of this study is to investigate whether PS-OCT and NIR reflectance imaging can be utilized to assess lesion structure in artificial enamel lesions on the smooth surfaces of primary teeth exposed to fluoride. The smooth coronal surfaces of primary teeth (n=25) were divided into 4 windows: sound, demineralization, demineralization with remineralization and APF with demineralization. Windows were treated with either acidulated phosphate fluoride (APF) for 1 minute, a demineralization solution for 4 days, and/or an acidic remineralization solution for 12 days. The samples were imaged using PS-OCT, QLF and NIR reflectance at 1400–1700 nm wavelengths. This study demonstrated that both PS-OCT and NIR reflectance imaging were suitable for assessing lesion structure in the smooth surfaces of primary dentition.

Keywords

Dental caries; primary teeth; lesion activity; remineralization; near-infrared imaging

1. INTRODUCTION

The primary tooth enamel is thinner in thickness and has less mineral content compared to permanent tooth enamel.[1] These differences in the chemical, morphological and physiological character between the primary and the permanent dentition can lead to differences in the rate of lesion progression and the penetration of near-infrared light.[2, 3]

Polarization-sensitive optical coherence tomography (PS-OCT) has been successfully used on both artificial and natural caries lesions to assess their severity and degree of remineralization.[4, 5] The optical changes associated with water loss have been exploited via quantitative light-induced fluorescence (QLF), thermal imaging and near-infrared (NIR) imaging.[6–8] NIR imaging can be used for caries detection since sound enamel is transparent in the NIR and the scattering coefficient increases exponentially with increasing mineral loss.[9] Lee et al. has demonstrated that NIR reflectance imaging at wavelengths longer than 1400 nm are well suited for the assessment of remineralization.[10]

Although the structural and chemical composition of primary and permanent tooth enamel vary, we hypothesize that PS-OCT and NIR reflectance imaging are capable of detecting changes in the degree of demineralization and remineralization in the enamel of primary

teeth. The objective of this work is to demonstrate that PS-OCT and NIR reflectance imaging methods can be used to monitor demineralization and remineralization on the smooth surfaces of primary tooth enamel.

2. MATERIALS AND METHODS

2.1 Sample preparation

Primary teeth (n=25) with sound smooth buccal or lingual enamel surfaces were selected that measured at least 8 mm in length and 4 mm in height. Each sample was partitioned into four windows by etching five thin fiducial lines 1.5 mm apart across the buccal or lingual enamel surface using a laser making 4 windows: sound, demineralization with remineralization, demineralization, and applied acidulated phosphate fluoride (APF) with demineralization. These fiducial lines were created by using a transverse excited atmospheric pressure (TEA) CO_2 laser, an Impact 2500, GSI Lumonics (Rugby, UK), operating at 9.3 μm with a pulse duration of 15 μs and a pulse repetition rate of 200 Hz. APF was carefully applied to the APF window for one minute and subsequent washing. A thin layer of acid-resistant varnish in the form of nail polish, Revlon (New York, NY), was applied to protect the sound and remineralization control windows before exposure to the demineralization solution. The samples with exposed demineralization windows were immersed in 45 mL aliquots of the demineralization solution for 4 days. The demineralization solution, which was maintained at 37°C and pH 4.5, was composed of 2.0 mmol/L calcium, 2.0 mmol/L phosphate and 0.075 mol/L acetate. After the demineralization period, the acid resistant varnish was removed by immersion in acetone in an ultrasonic bath for 15 minutes and the acid-resistant varnish was reapplied to the sound, demineralization, and APF with demineralization windows. The demineralization with remineralization windows were subsequently exposed to an acidic remineralization solution for 12 days. The acidic remineralization solution was composed of 4.1 mmol/L calcium, 15 mmol/L phosphate, 50 mmol/L lactic acid, 20 mmol/L HEPES buffer and 2 ppm F^- maintained at 37°C and a pH of 4.8. [11] After the 12 days of remineralization, the acid resistant varnish was removed and the samples were stored in 0.1 % thymol solution to prevent fungal and bacterial growth.

2.2 PS-OCT system

The PS-OCT system used in this study has been described previously. [5] An all fiber-based Optical Coherence Domain Reflectometry (OCDR) system with polarization maintaining (PM) optical fiber, high speed piezoelectric fiber-stretchers and two balanced InGaAs receivers that was designed and fabricated by Optiphase, Inc., (Van Nuys, CA) was used to acquire the images. [5] This two-channel system was integrated with a broadband superluminescent diode (SLD) DL-CS3159A, Denselight (Jessup, MD) and a high-speed XY-scanning motion controller system, ESP 300 controller with ILS100PP and 850GHS stages from Newport (Irvine, CA), for in vitro optical tomography. A high power (15 mW) polarized SLD source operated at a center wavelength of 1317 nm with a spectral bandwidth full-width-half-maximum (FWHM) of 84 nm was used to provide an axial resolution of 9 μm in air and 6 μm in enamel (refractive index = 1.6). Light from the sample arm was

focused onto the sample surface using a 20 mm focal length plano-convex lens providing a lateral resolution of approximately 20 μm.

The PS-OCT system was completely controlled using LabView™ software from National Instruments (Austin, TX). Each B-scan consisted of 300 A-scans spaced 50 mm apart. The A-scan sweep rate was 150 Hz with a dynamic range of 48 dB and each A-scan was an average of 10 scans. The total number of data points in each A-scan was 2000 over a scan range of approximately 5 mm in air.

2.3 Calculation of transparent surface layer thickness, lesion depth and integrated reflectivity (ΔR)

PS-OCT images were processed using a dedicated program constructed with LabView™ software. Image processing methods for surface layer detection and measurement method utilized an edge detection technique using the zero-crossing first-order derivative as described previously. [12]

Previous studies have shown that the integrated reflectivity, ΔR, over the estimated lesion depth positively correlates with the integrated mineral loss (volume percent mineral loss x μm), ΔZ. [13] ΔR was calculated by integrating from the base of the transparent layer through the entire estimated lesion body in the CP-OCT images. The transparent surface layer, lesion depth and ΔR measurements were estimated by averaging 25 A-scans from a 5×5 pixel region of interest.

2.4 Dehydration and NIR Reflectance Imaging

Each sample was placed in a mount connected to a high-speed XY-scanning motion controller system, Newport ESP 300 controller & 850G-HS stages coupled with air nozzles connected together to a compressed air and a light source. [10] Each sample was immersed in the water bath for 30 seconds while being vigorously shaken to enhance water diffusion. After the sample was removed from the water bath, the excess water on the surface of the lesion was removed with a disposable cotton roll. An image was captured as an initial reference image and the air spray was activated. Seven air nozzles were positioned 5 cm away from sample and the air pressure was set to 12 psi. Each measurement consisted of capturing a sequence of images at 4 frames per second for 30 seconds. The air nozzles and the light source were centered on the suspected lesion. The dehydration setup was completely automated using LabView™.

An Indigo Alpha near-infrared camera from FLIR Systems (Wilsonville, OR) with an InGaAs focal plane array, a spectral sensitivity range from 900 nm to 1750 nm, a resolution of 320 × 256 pixels and an InfiniMite™ lens from Infinity (Boulder, CO) was used to acquire all the images during the dehydration process. Light from a 150 W fiber-optic illuminator FOI-1 from E Licht Company (Denver, CO) was directed at the sample with crossed polarizers and a long-pass filter at 1400 nm (1400–1700 nm). Source to sample distance was fixed at 5 cm for all samples. Near-infrared reflectance images were processed and automatically analyzed using a dedicated program constructed with LabView™ software. The image contrast was calculated using $(I_L - I_S)/I_L$ for the final image (t = 30), where I_S is the intensity of the sound enamel and I_L is the intensity of the lesion. In addition

to lesion contrast, the intensity difference between the final and initial images, ΔI, was calculated using $I(t=30) - I_I$, where I(t=30) is the intensity at t = 30 seconds and I_I is the intensity prior to turning on the air nozzle. The overall growth rate (OGR) was calculated using the Levenberg-Marquardt algorithm. [10]

2.5 Fluorescence Imaging

A Dino-Lite digital microscope AM4115TW from AnMo Electronics (Hsinchu, Taiwan) with five blue LEDS at 480-nm for excitation and a 510-nm long pass filter was used to capture all the images after the dehydration process of the samples. The contrast ratio was calculated using $(Q_S - Q_L)/Q_S$, where Q_S is the intensity of the sound enamel and Q_L is the intensity of the lesion. [6]

2.6 Statistical Analysis

Sample groups were compared using repeated measures analysis of variance (ANOVA) with a Tukey–Kramer post hoc multiple comparison test. All statistical analyses were performed with 95% confidence with Prism™ from GraphPad software (San Diego, CA).

3. RESULTS AND DISCUSSION

Figure 1 shows the visible (A), PS-OCT integrated reflectivity (B), PS-OCT surface layer thickness (C), NIR reflectance (D), NIR intensity difference (E), and QLF contrast ratio (F) images with all 4 windows depicted of the same sample. Under visible light (Fig. 1A), it was difficult to distinguish windows from one another, which were treated with different solutions. Figure 1B and 1C demonstrate that PS-OCT is capable of discriminating sound primary tooth enamel from windows that have been exposed to different solutions. In addition, the PS-OCT was able to estimate the thickness of the highly mineralized surface layer to assess remineralization. The statistical analyses shown in Figs. 2A and 2B demonstrate that PS-OCT can detect the subtle increase in the surface layer thickness. It is interesting to note that most of the samples treated with the demineralization solution retained the surface layers. These natural primary teeth samples were exposed to the oral cavity and the surface of the enamel most likely contains high levels of acid resistant fluorapatite.

In Figs. 1D and 1E, NIR reflectance imaging highlights the demineralized primary tooth enamel in the demineralization window. The lesion measurements attained were highly variable due to structural variations, thus the intensity difference measurements were calculated to minimize this discrepancy. Figs. 2C – 2E show that NIR reflectance imaging was highly effective in assessing changes in the lesions in primary teeth, and the intensity difference measurement (Fig. 2D) was able to show a significant difference between the demineralization and the APF treated demineralization windows. Figures 1F and 2F show that QLF is also capable of detecting demineralization and remineralization in simulated primary tooth enamel lesions although it was not capable of detecting a significant difference between the demineralization and the APF treated demineralization windows. Our findings suggest that these novel optical imaging methods provide clinically useful

information such as lesion severity and presence of the highly mineralized surface layer, and these measurements can be utilized to assess the status of primary tooth enamel lesions.

Acknowledgments

The authors acknowledge the support of NIH/NIDCR Grants F30-DE23278, R01-DE17869 and R01-DE14698.

References

1. Mortimer KV. The relationship of deciduous enamel structure to dental disease. Caries Res. 1970; 4(3):206–223. [PubMed: 5270190]
2. Wang LJ, Tang R, Bonstein T, Bush P, Nancollas GH. Enamel demineralization in primary and permanent teeth. J Dent Res. 2006; 85(4):359–363. [PubMed: 16567559]
3. Pena, WA. MS Thesis. University of California; San Francisco, California: 2009. Optical Imaging of Early Dental Caries in Deciduous Teeth With Near-IR Light at 1310 nm.
4. Baumgartner A, Dicht S, Hitzenberger CK, Sattmann H, Robi B, Moritz A, Fercher AF, Sperr W. Polarization-sensitive optical optical coherence tomography of dental structures. Caries Res. 2000; 34:59–69. [PubMed: 10601786]
5. Fried D, Xie J, Shafi S, Featherstone JD, Breunig TM, Le C. Imaging caries lesions and lesion progression with polarization sensitive optical coherence tomography. J Biomed Opt. 2002; 7(4): 618–627. [PubMed: 12421130]
6. Ando M, Stookey GK, Zero DT. Ability of quantitative light-induced fluorescence (QLF) to assess the activity of white spot lesions during dehydration. Am J Dent. 2006; 19(1):15–18. [PubMed: 16555651]
7. Kaneko K, Matsuyama K, Nakashima S. Quantification of Early Carious Enamel Lesions by using an Infrared Camera. Early Detection of Dental Caries II. Annual Indiana Conference. 1999; 4:83–99.
8. Darling CL, Huynh GD, Fried D. Light scattering properties of natural and artificially demineralized dental enamel at 1310 nm. J Biomed Opt. 2006; 11(3):34023. [PubMed: 16822072]
9. Usenik P, Bürmen M, Fidler A, Pernuš F, Likar B. Near-infrared hyperspectral imaging of water evaporation dynamics for early detection of incipient caries. J Dent. 2014; 42(10):1242–1247. [PubMed: 25150104]
10. Lee RC, Darling CL, Fried D. Assessment of remineralization via measurement of dehydration rates with thermal and near-IR reflectance imaging. J Dent. 2015; 43(8):1032–1042. [PubMed: 25862275]
11. Yamazaki H, Margolis HC. Enhanced enamel remineralization under acidic conditions in vitro. J Dent Res. 2008; 87(6):569–574. [PubMed: 18502967]
12. Lee RC, Darling CL, Fried D. Assessment of remineralization via measurement of dehydration rates with thermal and near-IR reflectance imaging. J Dent. 2015; 43(8):1032–1042. [PubMed: 25862275]
13. Ngaotheppitak P, Darling CL, Fried D. Polarization Sensitive Optical Coherence Tomography for Measuring the Severity of Caries Lesions. Lasers Surg Med. 2005; 37(1):78–88. [PubMed: 15889402]

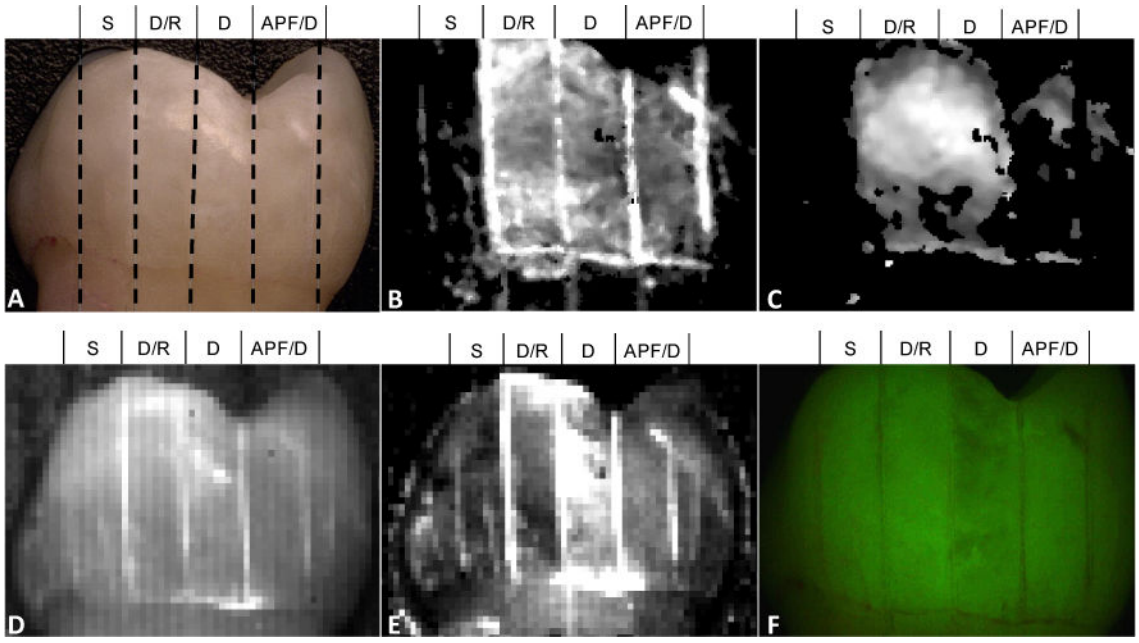

Fig. 1.

Visible (A), integrated reflectivity, ΔR (B) and surface layer thickness (C) measurements with PS-OCT, raw NIR reflectance (D), NIR intensity difference after dehydration (E) and QLF (F) images of a sample. Four windows (S: sound, D/R: demineralization with remineralization, D: demineralization, APF/D: APF with demineralization) are depicted for each image.

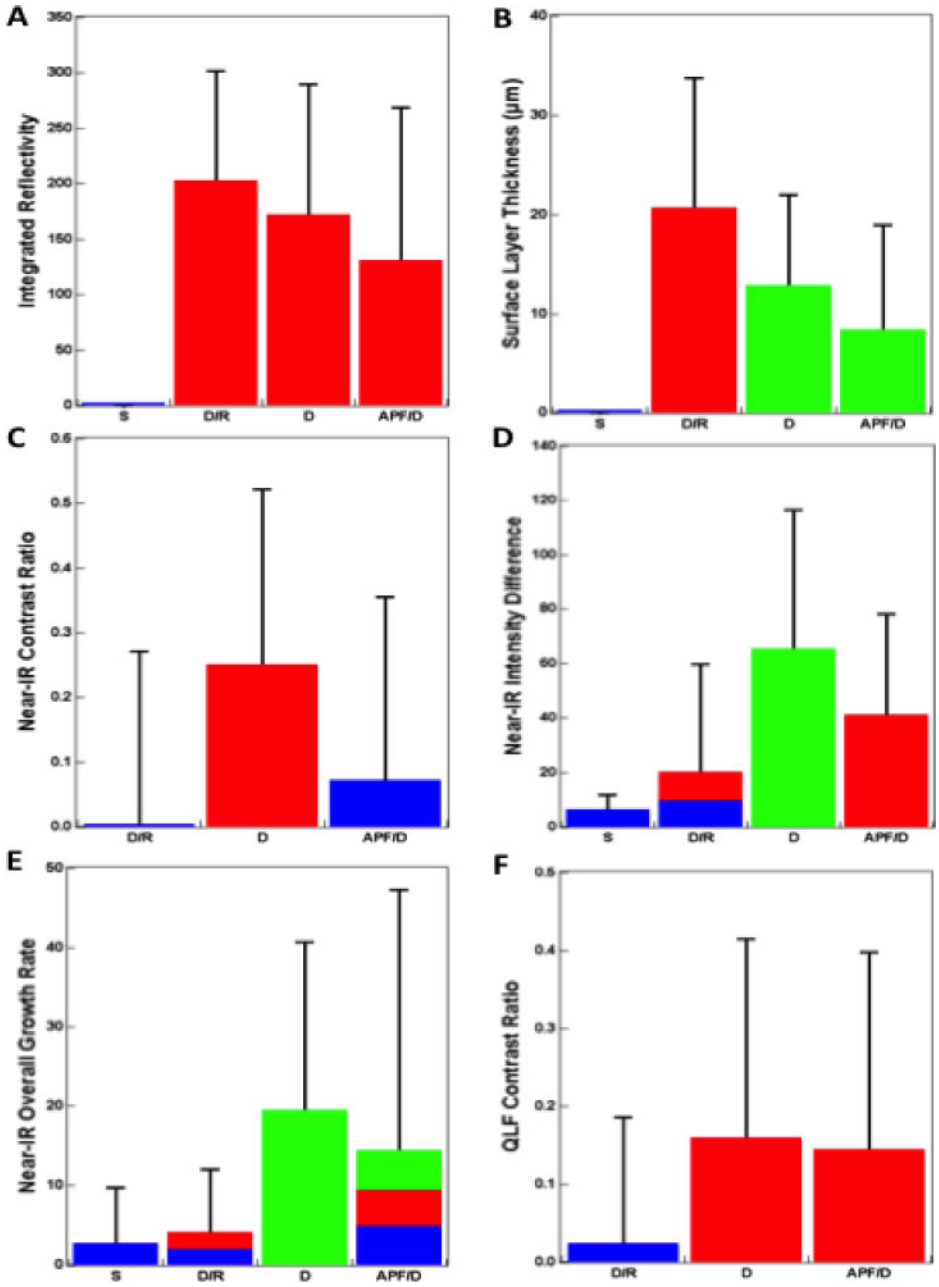

Fig. 2.

Mean ± S.D. of integrated reflectivity, ΔR (A), surface layer thickness (B) measurement with PS-OCT, NIR reflectance contrast ratio (C), NIR intensity difference (D), NIR overall growth rate and QLF contrast ratio (F). The following windows were compared: S (sound), D/R (demineralization with remineralization) D (demineralization) and APF/D (APF with demineralization). Bars not sharing any common colors are significantly different, $P < 0.05$ ($n = 25$).